Assessment of a phase change regenerator for batch industrial dryers

Gianluca Valenti, Alberto Seveso, Camilla Nicol Bonacina, and Abdullah Bamoshmoosh

View Online   Export Citation

Assessment of a phase change regenerator for batch industrial dryers

Gianluca Valenti[a], Alberto Seveso, Camilla Nicol Bonacina, and
Abdullah Bamoshmoosh

Politecnico di Milano, Dipartimento di Energia, Via R. Lambruschini 4A, 20156, Milano, ITALY.

[a]Corresponding author: gianluca.valenti@polimi.it

Abstract. Waste heat recovery in the industrial sector plays a major role for reducing the use of primary energy. This work assesses a phase change regenerator for heat recovery from industrial dryers operating in a batch mode. The chosen architecture is a fixed bed type consisting of two vertical stoves with horizontal rod bundles, each rode being a hollow steel cylinder filled with either of two paraffins selected from the market. A model was developed and implemented in MATLAB to describe the mass balances, the energy balances, the heat transfer coefficients, and the pressure drops of the flows and the cylinders within the stoves. The heat transfer coefficients can be computed for both non-condensing and condensing exhaust gas from the dryer. The phase change materials are modelled in a lumped parameter approach, while ambient air and wet exhaust gas via a simplified indirect method. For the case study of a real natural gas-fired batch dryer for cotton flat fabrics with an exhaust gas at 1 kg/s and at a temperature ranging from 40 to 140 °C, a parametric analysis is executed to identify trends and optimal configurations for the two paraffins. Then, a detail analysis is conducted on the temperature distribution for the flow and the cylinder within the stove for the hot and the cold blows. The paraffins with the higher fusion temperature at 118 °C is best. The regenerator 500 m wide and deep and 4 m high has an optimal configuration characterized by a cylinder diameter of 9 mm and a number of cylinder per row of 24, yielding an annual savings of 2260 euros. A regenerator with the same paraffin for all rows is not optimal as only the first and the last row change actually phase. Hence, the performance can be improved optimizing the selection of different paraffins along the rows.

INTRODUCTION

The worldwide energy use has been increasing continuously over the decades. The industrial sector alone consumes one-third of this global energy. According to the International Energy Agency [1], the adoption of energy-saving strategies within the sector could lead to a reduction in the use of primary sources from 18 to 26% with large benefits for the population and the environment. Among these strategies, waste heat recovery plays a major role.

Many studies on dryer heat recovery are available in literature, focusing though mainly on continuous dryers. The common technologies are heat exchangers and heat pumps, as explained by Bisharat and Krokida [2] who develop a powerful model to compare performances and costs of these technologies; their work shows that it is possible to achieve recoveries up to 40% with all the configurations. Ogulata [3] considers heat exchangers for continuous textile dryers and states that they are usually crossflow plate-type. Moreover, Anderson and Westerlund [4] compare a heat exchanger, a heat pump and an open absorption system for sawmill dryers; they conclude that heat exchangers are the most commonly used devices mainly because of their simplicity and low costs, despite their efficiency is low compared to heat pumps. They add that an absorption system is very interesting because it offers a good compromise between heat recovery and electricity consumption, with a 67.4% reduction of the heat demand and an electricity usage per year of 49.2 GWh against 1 TWh in the case of a heat pump. Jokiniemi *et al*. [5] perform a theoretical study and an experimental analysis in a scaled-down dryer for heat recovery in a recirculating batch grain dryer, concluding that a parallel plate heat exchanger offers a good solution reaching an 18% recovery. Minea [6] describes a wood drying heat pump with an optional natural-gas heater; this study provides data about the dehumidification energy costs and time for different operation modes and reports a reduction in the total energy consumption between 42% and 48%.

Phase change materials can store a large quantity of energy per unit volume when their latent heat is exploited. Solid-liquid phase change materials are the most suitable choice for regenerators because of their low specific volume change, as stated by Tabrizi and Sandrameli [7]. Sharma *et al*. [8] declare that the large amount of available phase change materials operating in a wide range of temperatures is another advantage; they classify these materials as organic, inorganic and eutectic. Organics are further divided into paraffins and non-paraffins. The formers are preferred commonly because they are non-corrosive, predictable, chemically stable below 500 °C, rather inexpensive, as well as they show a low volume change and have no supercooling issues. On the other hand, their main disadvantages are low thermal conductivity and flammability. Inorganics are classified as salt hydrates and metallics. Salt hydrates are characterized by high latent heat of fusion and high thermal conductivity with respect to paraffins. However, supercooling, the incongruent melting, and their corrosiveness make these phase change materials not suitable for all industrial applications. Metallics are less studied as phase change technologies because of their weight and cost. In their turn, eutectics are minimum-melting combinations of more components. They cover a wide range of temperatures and can be characterized by a wide variety of properties; however, their data are not readily available.

Lastly, thermal enhancement may make phase change materials more efficient. Qureshi *et al*. [9] analyze a number of techniques to increase the thermal conductivity. They show that metallic foams are generally preferred to nanoparticle inclusions because they assure good stability and high thermal conductivity. Moreover, they report that expanded graphite techniques allow for thermal conductivity enhancement ratios up to 45.

This work assesses a phase change regenerator for heat recovery from industrial dryers operating specifically in a batch mode. A regenerator is selected instead of a recuperator because it functions inherently in a batch mode too. The chosen architecture is a fixed bed type consisting of two vertical stoves that work in an alternating manner. The exhaust gas from the dryer flows downward in one stove during the hot blow, while the fresh air upward in the other stove during the cold blow. The downward hot blow transfers its energy to the stove bed, which will preheat the upward fresh air during the next cycle. The stove feeds are switched each cycle to make the process continuous. The stove beds are made of horizontal rod bundles. This structure is selected to ease the cleaning operations. Moreover, it is compatible with modular design and construction. The bundles can be arranged in either an aligned or a staggered configuration. The rods of the bundles are hollow cylinders filled with a phase change material.

The goal of this work is predicting the recoverable energy and the annual saving with either of two phase change materials selected on market. The methodology comprises the development of a mathematical model for mass balances, energy balances, heat transfer coefficients and pressure drops. The model is discretized in time as well as in space, implemented in MATLAB, and used to evaluate the application to a real case study. Rod bundle regenerators with phase change materials are uncommon in the literature and their application to batch drying seems unique.

The following sections describe the models employed in the work, the case study adopted to assess the regenerator, the parametric analysis to identify its optimal configuration with either of two materials, and the conclusions.

MODELS

This section describes the balances on the flow side, the heat transfer correlations, the phase change material relations, and the wet exhaust thermodynamic and transport properties. The exhaust gas is approximated here as wet air.

Flow-side balances

The compressibility effect and the thermal capacity of the flow side of the regenerator can be neglected. Therefore, the mass and energy balances of the flow side between the inlet and outlet of each row are simplified as

$$\frac{dm_{flw}}{dt} = \dot{m}_{in} - \dot{m}_{out} = 0 \tag{1}$$

$$\dot{Q}^{\rightarrow} = \dot{m}_{flw}(h_{flw,out} - h_{flw,in}) \tag{2}$$

where m_{flw} (kg) is the mass of the flow within the control volume, t (s) the time, $\dot{m}_{flw}$ (kg/s) the mass flow rate, h_{flw} (J/kg) the flow specific enthalpy, and $\dot{Q}^{\rightarrow}$ (W) the thermal power positive if transferred from the cylinders to the flow. In particular, the subscripts "in" and "out" stand for inlet and outlet, respectively, while "flw" for flow.

The pressure drop is computed via the correlation by Zukauskas [10] from the averaged Euler number Eu (-) as

$$Eu = k_1 \sum \frac{C_i}{Re_{max}^i} \tag{3}$$

where "max" indicates that the Reynolds number is calculated for the maximum velocity of the flow. The coefficients C_i (-) and k_1 (-) depend on the Reynolds number and the dimensionless pitches $a = S_T/D$ (-) and $b = S_L/D$ (-), where S_T (m) and S_L (m) are the vertical and longitudinal distance between the cylinders, respectively. The coefficient k_1 is different from 1 in the case of either non-square aligned or non-equilateral staggered rod bundle. Furthermore, k_i (-) corrections can be added in case of different geometrical characteristics and peculiar variations in fluid properties. The values of these coefficients are in the work by Zukauskas [10]. Finally, the total pressure drop ΔP_{tot} (Pa) is

$$\Delta P_{tot} = N_S \frac{1}{2} V_{max}^2 Eu \tag{4}$$

where N_S is the total number of rows in the stove and V_{max} (m/s) the maximum velocity of the flow.

Heat Transfer

Two possibilities for the heat transfer are considered: non-condensing and condensing exhaust gases. In the first case of only sensible heat transfer, an averaged Nusselt number, $Nu = \alpha L_c/\lambda$ (-), is calculated row by row as function of the Reynolds and Prandtl numbers, $Re = \rho V_c L_c/\mu$ (-) and $Pr = \mu c_p/\lambda$ (-), where α (W/(m^2 K)) is the heat transfer coefficient, L_c (m) the characteristic length, λ (W/(m K)) the thermal conductivity, ρ (kg/m^3) the fluid density, V_c (m/s) the characteristic velocity, μ (Pa s) the dynamic viscosity, and c_p (J/(kg K)) the heat capacity at constant pressure. The averaged Nusselt number $\overline{Nu}_D$ (-) is computed via the correlation by Zukauskas [11] as

$$\overline{Nu}_D = C\, Re_{D,max}^m\, Pr^{0.36} \left[\frac{Pr(T_{flw})}{Pr(T_{cln})}\right]^{1/4} \tag{5}$$

$$\begin{cases} 0.7 < Pr < 5000 \\ 10 < Re < 10^6 \\ N_S > 20 \end{cases} \tag{6}$$

where C (-) and m (-) coefficients depending on $Re_{D,max}$. The values of these coefficients are in the work by Zukauskas [11]. Then, the sensible heat transfer coefficient α_s (W/m^2 K) is found from the Nusselt number definition.

In the case of condensing exhaust gas, the calculation of the global heat transfer coefficient starts from the sensible coefficient analysis. A Lewis analogy is used to perform the mass transfer calculations that enables to obtain the values of condensing mass flow and corresponding total heat transfer. Therefore, the case of pure vapor condensation is first analyzed. Then, the model is refined considering the diffusion of the condensing vapor into the incondensable gases adopting the film method. The heat transfer coefficient α_c (W/(m^2 K)) and the mass flux of condensate m_{cond}'' (kg/(m^2 s)) are calculated as

$$\alpha_c = 0.728 \left[\frac{\lambda_l^3\, \rho_l\, \Delta\rho\, g\, h_{lv}}{\mu_l\, D\, (T_{flw}\text{-}T_s)}\right]^{1/4} \tag{7}$$

$$m_{cond}'' = \frac{\alpha_c(T_{flw}\text{-}T_{cln})}{h_{lv}} \tag{8}$$

where "l" stands for liquid phase, g (m/s^2) is the gravitational acceleration, and h_{lv} (J/kg) the enthalpy of condensation. Nusselt developed the solution in Eqq.(7) and (8) for pure stagnant vapor condensing a gravity-driven laminar liquid film under several simplifications. Hence, it is possible to refine the solution considering convection phenomena inside the condensate layer, as well as gravity and shear-stress effects. Accordingly, all the properties are calculated at the film temperature T_{film} (K) defined as

$$T_{film} = T_{cln} + 0.25(T_{flw}\text{-}T_{cln}) \tag{9}$$

A boundary layer between the bulk and the film condensate is considered when dealing with the film method. An energy balance is performed between the cylinders and the flow at the liquid film interface as

$$\dot{m}_v''\, h_{lv} + \alpha_s^*(T_b\text{-}T_i) = \alpha_c(T_i\text{-}T_{cln}) \tag{10}$$

where $\dot{m}_v''$ (kg/(m^2 s)) is the condensate mass flux, h_{lv} (J/kg) the latent liquid-vapor enthalpy and α_c is calculated substituting T_{flw} with T_i in Eq.(7). The subscripts "b" and "i" stand for the bulk and the interface, respectively.

The condensate mass flux $\dot{m}_v^{"}$ (kg/(m2 s)) is obtained integrating the Fick's law over the diffusion layer and rearranging it in terms of mass fluxes and pressures as

$$\dot{m}_v^{"} = \rho_b \alpha_m \ln\left(\frac{P-P_{v,i}}{P-P_{v,b}}\right) \tag{11}$$

The corresponding heat flux q_{lat} (W/m²) and the total heat flux q_T (W/m2) are calculated as

$$q_{lat} = \dot{m}_v^{"} h_{lv} \tag{12}$$

$$q_T = \dot{m}_v^{"} h_{lv} + \alpha_s^*(T_b - T_i) \tag{13}$$

where "lat" stands for latent. The modified heat transfer coefficient α_s^* (W/(m² K)) and the mass transfer coefficient α_m (m/s) are calculated as

$$\begin{cases} \alpha_m = \dfrac{D_{vg}}{\delta v} \\ \alpha_m = \alpha_s\left(\dfrac{Le^{2/3}}{\rho_b\, c_{p,b}}\right) \end{cases} \tag{14}$$

$$\begin{cases} \alpha_s^* = \alpha_s\left[\dfrac{a}{1-\exp(-a)}\right] \\ a = \dfrac{\dot{m}_v^{"}\, c_{p,b}}{\alpha_s} \end{cases} \tag{15}$$

where D_{vg} (m2/s) is the diffusion of vapor in gas, δv (m) is the diffusion layer thickness, while $Le = Pr/Sc$ (-), $Pr = \mu_b\, c_{p,b}/\lambda_b$ (-) and $Sc = \mu_b/\rho_b\, D_{vg}$ (-) are the Lewis, Prandtl and Schmidt numbers, respectively.

Phase Change Materials

Cylinders with a phase change material are modelled in a lumped parameter approach. Therefore, the cylinder energy balance is as

$$m_{cln} c_{cln} \frac{\partial T_{cln}}{\partial t} = \alpha_{flw} S_{cln}(T_{flw} - T_{cln}) \tag{16}$$

where m_{cln} (kg) is the cylinder mass, c_{cln} (J/(kg K)) the specific heat capacity of the cylinders, and S_{cln} (m²) the cylinder external surface. The final temperature of the cylinders is obtained integrating Eq.(16) over a time-step $(t_i - t_f)$ and rearranging it as

$$T_{cln}(t_f) = T_{flw} + [T_{cln}(t_i) - T_{flw}]e^{(-\frac{t_f-t_i}{\tau})} \tag{17}$$

where $\tau = \alpha_{flw}/\rho_{cln} c_{cln} L_c$ (s) is the time constant and $L_c = V_{cln}/S_{cln}$ (m) the characteristic length. The calculation of the absorbed energy $E_{cln}^{\leftarrow}$ (J) in Eq.(18) is used to find the melted fraction f (-) during the phase change transition through the inverse form of Eq.(19)

$$E_{cln}^{\leftarrow} = m_{cln} c_{cln}[T_{cln}(t_f) - T_{cln}(t_i)] \tag{18}$$

$$E_{cln}^{\leftarrow} = m_{cln} h_{ls}[f(t_f) - f(t_i)] \tag{19}$$

where h_{ls} (J/kg) is the latent enthalpy of liquid-solid transition. This simple model is accurate when the heat transfer resistance is very small, which is verified for a low Biot number

$$Bi = \frac{\alpha_{flw} L_c}{\lambda_{cln}} < 0.1 \tag{20}$$

If the relation of Eq.(20) is not valid, it is possible to add a characteristic resistance R_c (m² K/W) as in Eq.(21), and substitute α_{flw} with a global heat transfer coefficient α_g (W/(m² K)) in the definition of τ

$$R_c = k\frac{L_c}{\lambda_{cln}} \tag{21}$$

$$\alpha_g = \frac{1}{\alpha_{flw}} + R_c \tag{22}$$

where k (-) is an additional correction coefficient included if specific data from specific results are available. In this work, the k coefficient is set equal to 0.5. The resistance for the thin cylindrical casing R_{wrap} (m^2 K/W) is included as

$$R_{wrap} = \frac{\log(D_{ext} / D_{int})\, D_{ext}}{2\, \lambda_{wrap}} \tag{23}$$

where D_{ext} (m) and D_{int} (m) are the external and internal diameter of the steel casing, respectively.

Discretization

The stoves are discretized spatially on the vertical direction, identifying the N_S rows with the letter "s", and the inlet and outlet conditions of the flow at each row with "s - 1/2" and "s + 1/2", respectively. The time is discretized by N_t time-steps in the order of 0.1 s to ensure an acceptable accuracy in the implementation. From the point of view of the flow side, Eqq.(1) and (2) can be reformulated respectively for each row as

$$\dot{m}^s_{s-1/2} = \dot{m}^s_{s+1/2} \tag{24}$$

$$\dot{Q}^{s\rightarrow} = \dot{m}^s(h_{flw,s+1/2} - h_{flw,s-1/2}) \tag{25}$$

while from the point of view of the cylinder side, the cylinder radius is not discretized and a single cylinder temperature is the result solving Eqq.(16) to (23) for each row and each time-step.

Resolution and implementation

Given the initial and boundary conditions, the properties of the flow are calculated at the inlet of each row. The heat transfer coefficient is obtained. Then, the temperature of the cylinders is computed and used to calculate the thermal power exchanged by the row. The flow temperature and enthalpy at the outlet of the row are computed coupling Eq.(25) with the exchanged thermal power. This procedure is repeated row-by-row over each time-step of the cycle.

The model is implemented in a MATLAB parallel code that solves the two stoves simultaneously. Because the regime temperature of the cylinders is not known at the beginning, a uniform initial temperature is set. Therefore, a cyclic approach is executed until a steady-state condition is reached in both stoves. The user must set the geometric parameters of the stoves, the initial as well as boundary conditions of the flow and the initial temperature of cylinders. The user should also set a temporal discretization grid that ensures good accuracy of the numerical results.

Ambient air and wet exhaust gas

The wet exhaust gas is approximated as wet air. Ambient and wet air are modelled as mixture of nitrogen, oxygen, argon and water. Vapor-liquid equilibrium is assessed through an indirect method. Ideal gas behavior is considered for the vapor phase and an activity coefficient equal to 1 for the liquid phase. Poynting factors are neglected for the liquid phase. This simple and fast model proves differences averagely below 0.5% in the region of interest with respect to the Peng-Robinson and the Peng-Robinson-Strijek-Vera equations of state [12].

Thermodynamic properties of the vapor phase are calculated coherently through the ideal gas law. Single component molar properties are calculated and weighted on molar composition. Specific heat of each component is calculated through the fourth order polynomial by Poling *et al*. [13]. Density of the liquid phase is calculated through the Rackett equation of state [14], while the specific heat through the corresponding state principle. Then, the specific heat is used to calculate the specific enthalpy of the liquid phase.

Transport properties are calculated accordingly to the work by Chung *et al*. [15]. In their model, correlations based on the kinetic gas theory are used for calculating dynamic viscosity and thermal conductivity. Dilute gas viscosity is calculated through the Chapman-Eskong theory. Solution of these models represent the properties of low pressure systems. A corrective factor is then introduced for condensed phases and high pressure systems. These corrections are based on the reduced value of the specific volume employing empirical correlations developed to extend the kinetic gas theory model to include condensed phases of common interest, including polar and associating fluids.

CASE STUDY

The case study is a real natural gas-fired batch dryer for cotton flat fabrics, like bed linens or tablecloths, in an industrial laundry serving hotels and restaurants. The dryer has a nominal load of 85 kg, referred to the dry fabric, and a cycle time of 20-22 minutes, including loading, drying, cooling and unloading the fabrics. During the drying process, lasting 15 to 17 minutes, the temperature of the fabric, the air inlet to the dryer from the burner and the exhaust from the dryer are measured continuously. Fig.1 shows typical values of these temperatures. The shown temperature of the exhaust is used in this work. In contrast, flow rate and humidity of the exhaust instead are not measured. Here, a mass flow rate of 1 kg/s at an absolute humidity of 0.04 kg of water per kg of dry air is taken from a preliminary estimation.
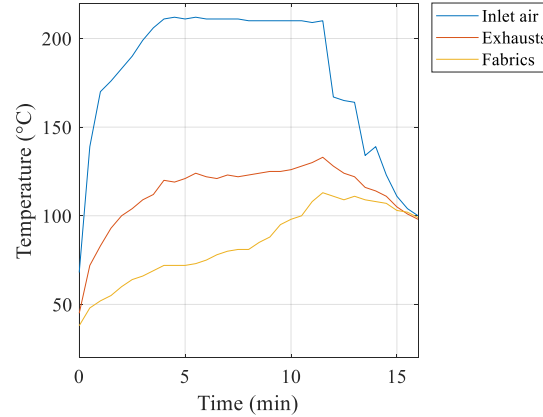

FIGURE 1. Measured temperatures of the fabric, the air inlet from the burner and the exhausts from the dryer during a typical cycle of the dryer considered in this work.

The stoves are assumed to have a squared cross area designed to ensure a flow velocity between 3 and 5 m/s, as a compromise between heat transfer and pressure drop. Width and depth of the stove are taken at 500 mm, while the height at 4 m in order to exploit as much as possible the available space next to the dryer. The dimensionless vertical pitch b is taken equal to 2, which is an average value for the adopted correlations. Instead, diameter of the cylinders and number of cylinders per row are analyzed parametrically. When a diameter and a number per row are selected, the number of rows in each stove is calculated from b in order to fill the whole height of the regenerator. To reduce the computational time, which tends to be high, the parametric analysis is performing excluding water condensation.

Two distinct paraffins are selected from the market: "A82" and "A118" by PCM Products Ltd [16]. Tab.1 reports the following properties: fusion temperature, latent heat of phase transition, specific heat, density, and thermal conductivity. The thermal conductivity of paraffin "A118" is taken equal to that of "A82" because not available in the literature. The parametric analysis is performed for both paraffins to identify trends and optimal configurations.

TABLE 1. Properties of the selected paraffins from the market by PCM Products Ltd [16]

Properties	A82	A118
Fusion temperature (°C)	82	118
Latent heat (J/kg)	170000	285000
Specific heat (J/(kg K))	2210	2700
Density (kg/m³)	850	1450
Thermal conductivity (W/(m K))	0.22	0.22 (assumed)

The energy indexes are the mass specific recovery (kJ/kg) and the pumping work specific recovery (kJ/kJ), that are the ratios of the energy recovered, $E_{recovered}$ (kWh), with respect to the total mass of the stove and to the pumping work, respectively. In addition, the adopted economic index is the annual saving C_{saving} (€/year) as

$$C_{saving} = n_{cycles} \left(\frac{E_{recovered} C_{gasnat}}{\eta_{brn}} - 2 \frac{E_{fan} C_{electric}}{\eta_{fan}} \right) \qquad (26)$$

where n_{cycles} is the number of cycles per year, C_{gasnat} (€/kWh) the natural gas cost, E_{fan} (kWh) the energy spent ideally for the fans per stove in one cycle, $C_{electric}$(€/kWh) the electricity cost, whereas η_{brn} (-) as well as η_{fan}(-) are reference burner and fan efficiencies, respectively. The cost of the pumping work is multiplied by 2 because two fans are necessary, while only the energy recovered in the stove crossed by the cold blow is exploited. The reference burner efficiency comprises the thermal loss and considers that a fraction of the heating value of the natural gas is lost as hot exhaust gas. Tab.2 reports the adopted values of all parameters in Eq.(26).

TABLE 2. Adopted values of the parameters to evaluate the annual saving C_{saving} (€/year)

n_{cycles}	C_{gasnat} (€/kWh)	$C_{electric}$ (€/kWh)	η_{brn} (-)	η_{fan}(-)
6000	0.047	0.18	0.9	0.7

At last, the optimal configuration in terms of annual saving found in the parametric analysis is simulated in detail including water condensation. For this case, the temperatures of the cylinders and the flow along the stoves at steady-state conditions are investigated for both the hot and cold blows.

RESULTS

This section describes the results for the parametric analysis as well as the optimal configuration analysis.

Parametric analysis

Figg.2(a) and 3(a) show the mass specific recovery (kJ/kg) and the pumping work specific recovery (kJ/kJ) for parametric values of the diameter of the cylinders in case of paraffins "A118" and "A82". Along each curve the number of cylinders per row varies. The sharp change in slope of the curves is due to the different increase rates of the pumping work and energy recovery while increasing the number of cylinders per row. Hence, the pumping work specific energy recovery is characterized by a maximum in correspondence to the optimal configuration for a certain diameter. For a specific configuration, paraffin "A82" ensures higher mass specific energy recoveries because its density is lower. However, it is characterized by lower pumping work specific energy recoveries because the recovery percentage is lower with respect to paraffin "A118", while the pumping work is not affected by the material adopted.

Similarly, Figg.2(b) and 3(b) show the annual savings and the number of cylinder per row. Paraffin "A118" achieves the highest energy saving per year with a cylinder diameter of 9 mm and a number of cylinders per row of 25. Specifically, they show that 3690 euros per year are saved with a corresponding specific energy recovery of 223 kJ/kg. An optimal value of the saving per year for each cylinder diameter is present because the pumping energy and the energy recovery increase at different rates while increasing the number of cylinders per row. Moreover, the smaller the rod diameter, the higher the energy saving due to the low thermal conductivity of paraffins.

Optimal configuration analysis

Overall, the optimal configuration in terms of energy savings is found for paraffin "A118" with a cylinder diameter of 9 mm and a number of cylinders per row of 25. This configuration is selected to study in detail the operating conditions of the regenerator. Figg.4(a) and 5(a) show the temperature of the first, middle and last rows over time for the hot and cold blows. The cylinders are characterized by phase change transition only in the first and last rows of the stove for the hot and cold blow, respectively. Moreover, the decreasing flow temperature for the hot blow and the increasing flow temperature for the cold blow along the regenerator make less effective the energy exchange in the last rows. Hence, different paraffins in different rows may be adopted to optimize the heat exchange process.
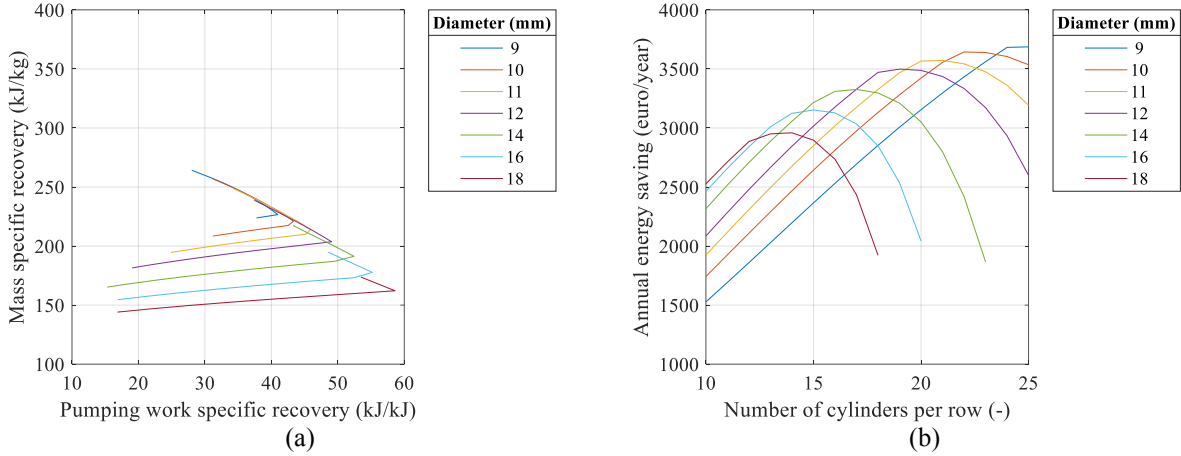
FIGURE 2. Results of the parametric analysis for paraffin "A118". Fig.(a) depicts the mass specific recovery versus the pumping work specific recovery. Fig.(b) shows the annual saving for different configurations.
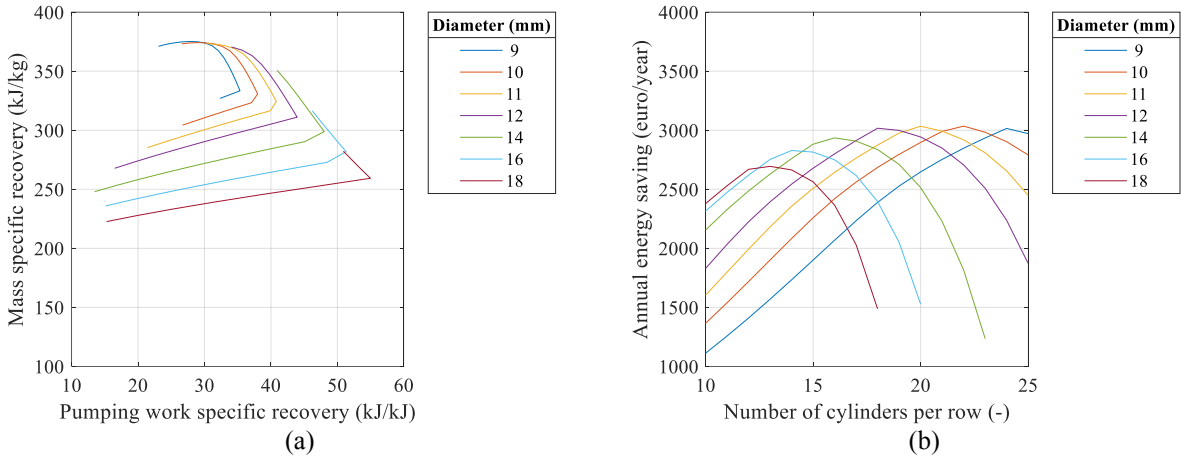

FIGURE 3. Results of the parametric analysis for paraffin "A82". Fig.(a) depicts the mass specific recovery versus the pumping work specific recovery. Fig.(b) shows the annual saving for different configurations.

Fig.4(b) shows the temperature of the hot blow along the regenerator for different instants. The peculiar curves for the initial and final time-steps are due to the low air inlet temperature at the beginning and at the end of the dryer cycle. Indeed, the cylinders in the first rows are warmer than the flow and, hence, the air temperature slightly increases at the inlet of the regenerator. In the middle phase of the cycle, the flow temperature decrease across the stove is much higher, depicting higher effectiveness in the heat transfer. Moreover, the outlet flow temperatures are lower at the beginning of the cycle because the phase change material matrix is not saturated yet, and higher differences in temperature between the flow and the matrix are present. At the very end, the difference between the air inlet temperature and the outlet one must be as high as possible to exploit the flow energy in the most effective way.

Lastly, Fig.5(b) depicts the flow temperature along the regenerator for the cold blow and, in particular, the temperature of the preheated air at the inlet of the dryer. Temperature distributions for different instants are quite similar because the regenerator inlet air temperature is constant and equal to 20 °C. The outlet flow temperatures are higher at the beginning of the cycle because more energy is transferred from the cylinders to the blow, similarly to the hot blow: the temperature difference between the inlet and outlet of the stove is 100 °C and 20 °C for the initial and final instants, respectively. However, the outlet temperatures during the cold blow in the last phase of the cycle could be increased adopting phase change materials in the last rows with transition temperatures lower than in the first rows.
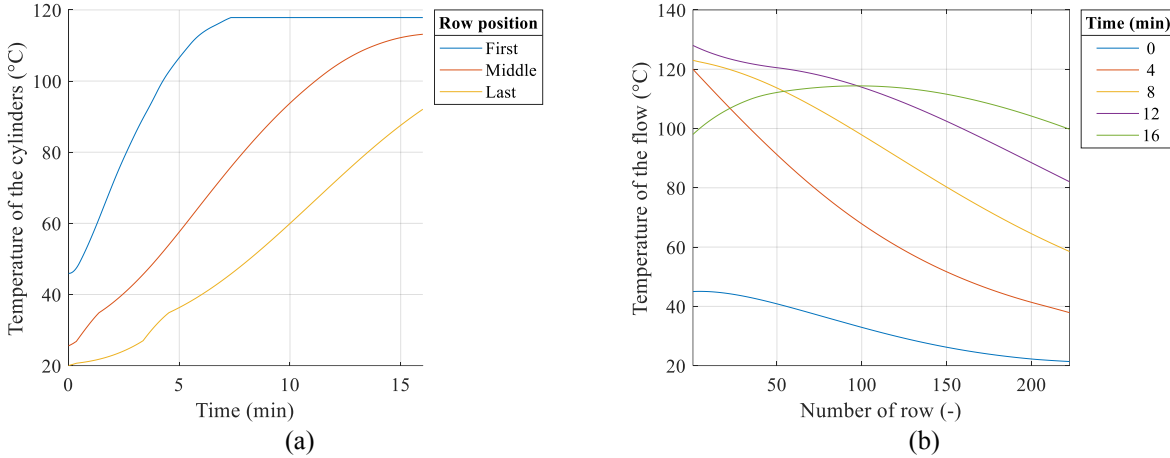
FIGURE 4. Temperature distributions for the hot blow. Fig.(a) depicts the cylinder temperature for the first, middle and last row over time. Fig.(b) depicts the flow temperature across the stove for 5 different instants of the cycle.

FIGURE 5. Temperature distributions for the cold blow. Fig.(a) depicts the cylinder temperature for the first, middle and last row over time. Fig.(b) depicts the flow temperature across the stove for 5 different instants of the cycle.
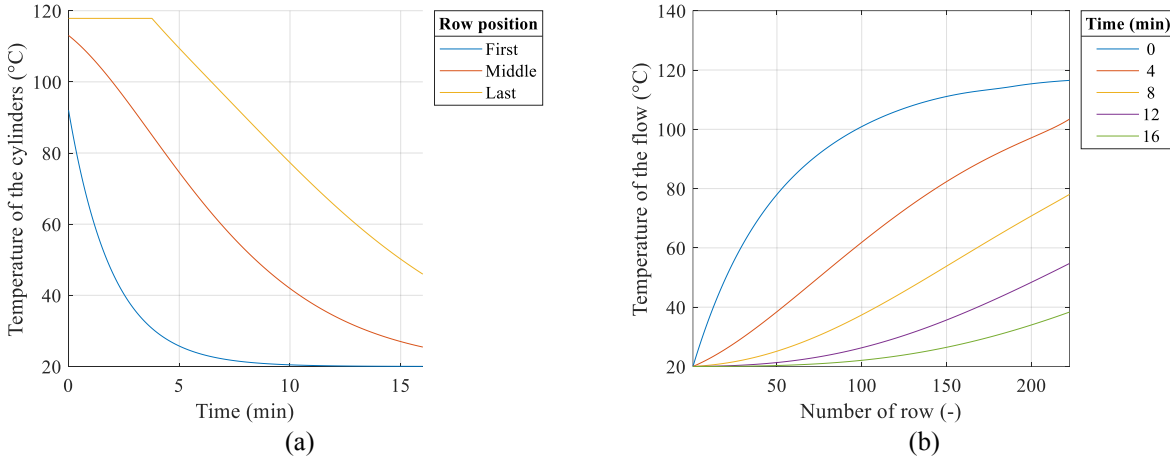
CONCLUSIONS

This work assesses a phase change regenerator for heat recovery applied to a real case study of an industrial dryers operating in a batch mode. The regenerator fixed beds are made of horizontal rod bundles, each rod being a hollow steel cylinder filled with either of two phase change paraffins selected from the market. The conclusions are as follows.

- A model was developed and implemented in MATLAB to describe the mass balances, the energy balances, the heat transfer coefficients, and the pressure drops of the flows and the cylinders within the stoves.
- For a given diameter of the cylinder, the energy recovery with respect to the total mass of the stove and to the pumping energy as well as the annual saving show an optimal value. This trend is similar for the two paraffins.
- For the case study with a hot blow at 1 kg/s and a temperature ranging from 40 to 140 °C with the maximum at about 12 minutes over a cycle of 16 minutes, the paraffin with a fusion temperature of 118 °C is best.
- The regenerator 500 m wide and deep and 4 m high has an optimal configuration characterized by a cylinder diameter of 9 mm and a number of cylinders per row of 25, yielding an annual savings of 3690 euros.
- A regenerator with the same paraffin for all rows is not optimal as only the first and the last row change phase.

The future work will focus on measuring the flow rate and the humidity of the real case dryer and optimizing the selection of different paraffins along the rows.

REFERENCES

[1]   International Energy Agency, "Tracking industrial energy efficiency and CO2 emissions," 2007.

[2]   G. I. Bisharat and M. K. Krokida, "Heat recovery from dryer exhaust air," vol. 22, no. 7, pp. 1661-1674, 2004.

[3]   R. T. Ogulata, "Utilization of waste-heat recovery in textile drying," *Applied Energy,* vol. 79, pp. 41-49, 2004.

[4]   A. Jan-Olof and W. Lars, "Improved energy efficiency in sawmill drying system," *Applied Thermal Engineering,* vol. 113, pp. 891-901, 2013.

[5]   J. Tapani, H. Mikko, O. Timo and A. Jukka, "Parallel plate heat exchanger for heat energy recovery in a farm grain dryer," *Drying Technology,* vol. 34, no. 5, pp. 547-556, 2016.

[6]   V. Minea, "Efficient Energy Recovery with Wood Drying Heat Pumps," *Drying Technology,* vol. 30, no. 14, pp. 1630-1643, 2012.

[7]   N. Tabrizi and M. Sadrameli, "Modelling and simulation of cyclic thermal regenerators utilizing encapsulated phase change materials (pcms)," *International Journal of Energy Research,* vol. 27, p. 431–440, 2003.

[8]   A. Sharma, V. Tyagi, C. Chen and D. Buddhi, "Review on thermal energy storage with phase change materials and applications," *Renewable and Sustainable Energy Reviews,* vol. 13, pp. 318-345, 2009.

[9]   H. M. M. Ali, S. Khushnood and Z. A. Qureshi, "Recent advances on thermal conductivity enhancement of phase change materials for energy storage system," *International Journal of Heat and Mass Transfer,* vol. 127, pp. 838-856, 2018.

[10] A. Zukauskas, "Banks of Plain and Finned Tubes," in *H.E.D.H.*, Schlunder, E.U., 1983.

[11] A. Zukauskas, "Heat transfer from tubes in crossflow," *Advances in Heat Transfer,* vol. 18, pp. 87-159, 1987.

[12] R. Strijek and J. H. Vera, "PRSV-An Improved Peng-Robinson Equation of State with New Mixing Rules for strongly Nonideal Mixtures," *The Canadian Journal of Chemical Engineering,* vol. 64, pp. 334-341, 1986.

[13] B. Poling, J. Prausnitz and J. O'Connell, The Properties of Gases and Liquids, McGraw-Hill, 2001.

[14] H. Rackett, "Equation of State for Saturated Liquids," *Journal of Chemical and Engineering Data,* vol. 15, no. 4, 1970.

[15] T.-H. Chung, M. Aljan, L. L. Lee and K. E. Starling, "Generalized Multiparameter Correlation for Nonpolar and Polar Fluid Transport Properties," *Industrial and Engineering Chemistry Research,* vol. 27, pp. 671-680, 1988.

[16] PCM Products Ltd, [Online]. Available: http://www.pcmproducts.net/. [Accessed 05 2019].